Physiol. Meas. **30** (2009) 129–140 doi:10.1088/0967-3334/30/2/002

Impedance-based tissue discrimination for needle guidance

Håvard Kalvøy[1,2,5], Lars Frich[3], Sverre Grimnes[1,2], Ørjan G Martinsen[1,2], Per Kristian Hol[3] and Audun Stubhaug[4]

[1] Department of Clinical and Biomedical Engineering, Rikshospitalet University Hospital, Sognsvannsveien 20, 0027 Oslo, Norway
[2] Department of Physics, University of Oslo, Norway
[3] The Interventional Centre, Rikshospitalet University Hospital, Oslo, Norway
[4] Department of Anaesthesiology, Rikshospitalet University Hospital, Oslo, Norway

E-mail: havard.kalvoy@fys.uio.no

Received 29 August 2008, accepted for publication 5 December 2008
Published 9 January 2009
Online at stacks.iop.org/PM/30/129

Abstract

Measurement of electrical impedance can discriminate between tissues of different electrical properties. A measurement system with adequate spatial resolution focused on a volume around the tip of a needle or other invasive clinical equipment can be used to determine in which type of tissue the tip is positioned. We have measured the sensitivity zone of a needle electrode with an active electrode area of 0.3 mm^2, and measured impedance spectra in porcine tissue *in vivo*. Small electrode impedance data will be influenced by electrode polarization impedance (EPI) at low frequencies. To refine existing methods for needle guidance with higher spatial resolution, we have used multivariate analysis and new interpretations of EPI, and tissue data gathered with selected needle electrodes. The focus of this study is on discrimination between muscle and fat/subdermis for drug administration, but our results also indicate that these refinements will facilitate new clinical applications for impedance-based needle guidance in general.

Keywords: impedance, needles, biological tissues, electrodes, sensitivity zone

1. Introduction

Different types of tissues are known to have different electrical impedance properties (Gabriel *et al* 1996a, 1996b, Foster and Schwan 1995, Schwan 1963, Faes *et al* 1999). If these properties are measurable and characteristic for tissue types, impedance measurements can be

[5] Author to whom any correspondence should be addressed.

used to distinguish between different types of tissue. In many clinical applications (e.g. drug administration, diagnostic and surgical procedures) differentiation between types of soft tissues and body compartments can be crucial. If local impedance measurements can determine the tissue type surrounding a needle tip, or the first surface part of any clinical equipment for invasive use, this can be used to *guide* an operator to the desired tissue or position. With adequate spatial resolution such a method could facilitate a wide range of clinical applications. Examples are biopsies and ablation in small volumes, or drug delivery transcutaneously into a vessel or a small volume of muscle, nerve or adipose tissue. An impedance-based method may be able to measure tissue differences not detectable with competing technologies, e.g. imaging modalities. Such a method can then enable smaller and more affordable easy-to-use devices and provide instantaneous feedback to the operator. Different methods and applications for impedance-guided positioning have been published earlier. Relevant examples are methods for ensuring catheter-tissue contact during RF ablation (Cao *et al* 2002, Cheung *et al* 2004, Johnson *et al* 2003), position guidance for a hypodermic needle (Dalamagas and Sapia 1993, Levendusky *et al* 2005, Stoianovici *et al* 2002, Hernandez *et al* 2001) and dental apex locators (Gordon and Chandler 2004). Due to the defined type of geometry in the apex of teeth and high impedance of teeth compared to the pulp tissue, apex locators can determine the depth of a root canal with a spatial resolution down to around 0.5 mm. Soft body tissues are generally quite inhomogeneous and have large geometrical variations (Grimnes and Martinsen 2008, chapter 4.2). The difference in electrical properties between such tissue types is much less than between teeth and pulp, so obtaining the same spatial resolution in these tissues is a more challenging task.

In general, the volume sensitivity of an impedance measurement will be a function of the square of the current density in a given tissue volume (Grimnes and Martinsen 2008, Malmivuo and Plonsey 1995). A truly unipolar measurement must have an electrode setup resulting in a high current density adjacent to the active electrode surface, compared to the rest of the tissue. In this way, the measured impedance will be dominated by the vicinity of the active electrode, and dependent on the area and geometry of this (Grimnes and Martinsen 2008, Salazar *et al* 2004, Kinouchi *et al* 1997). The impedance data will reflect some kind of averaging over the tissue in the dominant sensitivity volume (Kinouchi *et al* 1997). The smaller the active electrode area, the higher the obtained spatial resolution (Schwan 1963, Grimnes and Martinsen 2008). Grimnes and Martinsen (2008) have pointed out that for a hemispheric electrode in a homogenous medium, 90% of the measured resistance is due to the volume within a radius ten times the radius of the electrode. Cao *et al* (2002) found that for a spherical electrode with a radius of 1.25 mm, a unipolar impedance measurement was dominated by the volume within a 50 mm radius, and only 1.3% contribution was found in the volume between 50 mm and 100 mm distance from the electrode. Kinouchi *et al* (1997) estimated the sensitivity zone for a 0.5 mm diameter bevel tip needle with a plot of equipotential lines around a 0.5 mm diameter conical needle. They derived the 90% sensitivity zone to be inside a 7.6 mm diameter sphere.

All unipolar impedance measurements will be influenced by electrode polarization impedance (EPI). For a unipolar spherical electrode the ratio between EPI and tissue impedance is inversely proportional to the electrode radius (Grimnes and Martinsen 2008). Hence, the relative influence of EPI can be made negligibly small by using a sufficiently large electrode. But reduced electrode size for higher spatial resolution will enlarge the relative influence from EPI. For the electrode size described above, large influence from EPI can be expected at low frequencies (Schwan 1963, Stoianovici *et al* 2002, Mirtaheri *et al* 2005, Schwan 1992, 1966, Schwan and Kay 1956). Traditionally, EPI has been seen as a source of error that has lead to rejection of data, or that has to be removed before analysing the measurement data (Schwan

1992, Gabriel *et al* 1996b, Kinouchi *et al* 1997, Cao *et al* 2002). Many methods for elimination of EPI have been suggested earlier (Cao *et al* 2002, Kinouchi *et al* 1997, Schwan 1992, 1966, Schwan and Kay 1956). Cao *et al* (2002) recommended using measuring frequencies above 50 kHz to minimize EPI. Kinouchi *et al* (1997) reported a large influence of electrode polarization in their measurements in the frequency range up to 10 kHz. They estimated the EPI from measurements and subtracted it from their data. However, Schwan (1992, 1966) found that the EPI is dependent on cell concentration in a suspension. Thus it cannot be estimated for such use from measurements in another suspension. If the EPI is dependent on tissue type and not only the concentration of a suspension, subtraction of the EPI will be difficult. Our idea is that if tissue-dependent characteristics can be found in the EPI, this could also be used for tissue type discrimination. The main goal of this study was to determine the feasibility of discriminating between small tissue volumes in general (refer figure 6). But for one of our planned applications involving drug administration, we have our main focus on discriminating muscle tissue from fat and subdermis. The spatial resolution needed for such applications will require a 90% sensitivity zone inside a radius of 1–4 mm from the needle tip.

As described above, other investigators have found a high influence from EPI for frequencies up to 10–50 kHz in similar measurements. We are aiming at higher spatial resolution than reported by these and will have to use electrodes with a smaller active area and must expect even a higher influence from EPI reaching over a wider frequency range (Grimnes and Martinsen 2008, chapter 6.3.1). Feasibility determination has been done by finding needle electrodes with optimal spatial resolution, and by using multivariate analysis on porcine *in vivo* data gathered with these needles in the frequency range from 10 Hz to 1 MHz. This data will include both tissue data and EPI, and we will determine if such data can be used for tissue discrimination and needle guidance.

By exploiting these fundamentals we will determine the feasibility of refining current methods, and thus enable needle guidance with sufficient spatial resolution, by using needle electrodes with adequate size and introducing EPI data and multivariate analysis as new tools.

2. Materials and methods

2.1. Measurements

To determine the sensitivity zone around a needle tip, theoretical analysis was verified by *in vitro* impedance measurements in different tissue models. With knowledge of fundamental electrical properties of the needles, gathering *in vivo* impedance data was done on an anesthetized pig.

All measurements were unipolar measurements of complex impedance done with a Solartron 1260/1294-system ((2) in figures 1 and 2). To illustrate the measurement principles the Solartron parts have also been drawn with separate component blocks. Spectra were taken at frequencies from 10 Hz to 1 MHz (4 frequencies/decade), and constant frequency measurements were done at 100 kHz. All measurements were done with a constant voltage of 30 mV rms.

2.2. Needles

In this study, we used two types of insulated needles as measuring electrodes (active electrode). Both needle types were insulated except for the active electrode area determined by the exposed tip. In preliminary testing, various needles gave promising results, but for feasibility determination we limited this study to one solid and one hollow needle. Needle type 1 was

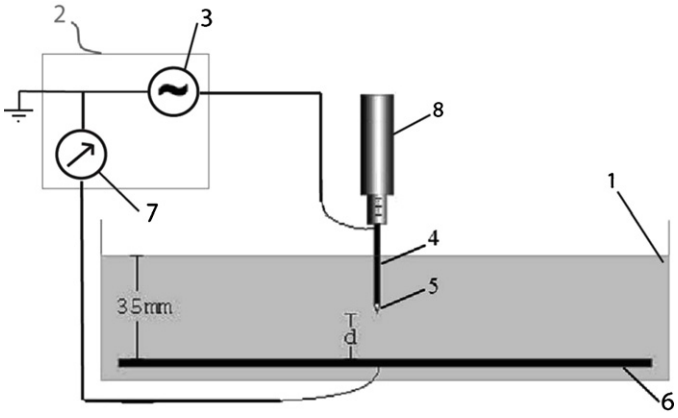

Figure 1. Two-electrode unipolar *in vitro* measurement setup with a small active electrode (5) and a large neutral electrode (6).

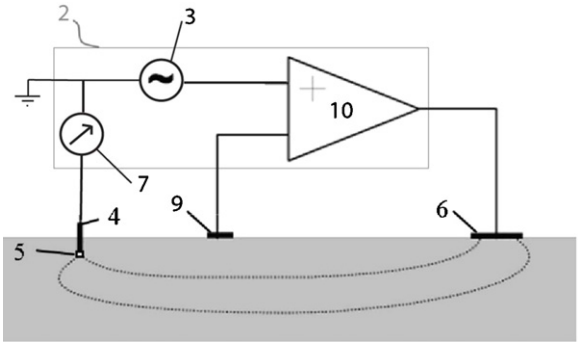

Figure 2. The principle of a three-electrode *in vivo* unipolar measurement setup. Current flows between electrodes (5) and (6), and electrode (9) is the reference electrode. The Solartron part of the system is indicated by the box marked (2).

a solid needle with a conical tip, 'Disposable Monopolar Needle Electrode, 37 × 0.33 mm' (REF 9013S0631, an active electrode area of 0.3 mm^2), from Medtronic A/S, Minneapolis, US. Needle type 2 was a hollow needle with a bevel cut tip, 'Stimuplex® A', 0.7 × 50 mm (REF 04894502, the active electrode area is not given) from B Braun Melsungen AG. All needles of type 1 were preconditioned with a cathodic constant current (1 μA in 1 min) in a sterilized saline bath (0.9% NaCl) before use. Such treatment had no noticeable effect on needle type 2, so they were not preconditioned.

2.3. In vitro

In the *in vitro* measurements the unipolarity was obtained by using a two-electrode setup with a large neutral electrode (shown in figure 1). This simple electrode configuration enables analytical solutions for the impedance calculation, and is easy to simulate in finite element (FEM) analysis software. An insulating tank (a bottom area of 150 × 210 mm, (1) in figure 1) was filled with saline (0.9% NaCl) to 35 mm height. The needle type 1 was used as an active electrode (5), and the counter electrode (6) was a stainless steel plate of 104 × 150 mm.

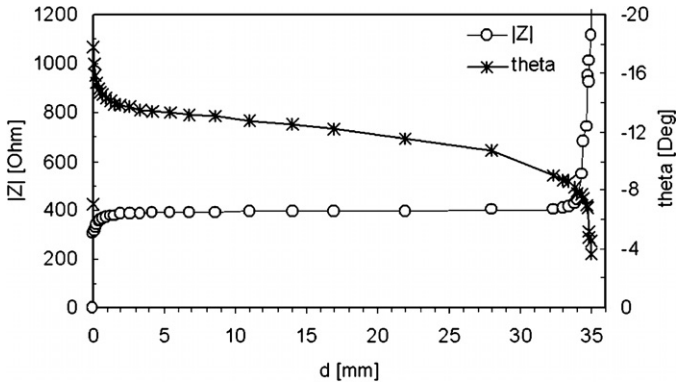

Figure 3. Impedance at 100 kHz measured with needle type 1 in the saline tank shown in figure 1. Above the saline surface (35 mm) there is air representing a volume with almost infinite impedance. In the other end (0 mm), the neutral electrode represents a volume with approximately zero impedance. The almost flat dependence between the needle position and modulus ($|Z|$) in the middle of the tank, and the abrupt change near the inhomogeneities, shows clearly that such an electrode setup is mainly sensitive to impedance changes a few millimetres from the active electrode at the needle tip.

By using a micrometer screw (8) the needle was moved from the bottom of the tank (0 mm, given from the counter electrode to the sharp end of the needle) and up to the surface of the saline (35 mm) in steps from 50 μm to 6 mm. The step size was the smallest close to the bottom and the top, and larger in the middle of the bath (the distribution of measuring points can be read from the x-axis in figure 3). At each distance from the bottom the impedance at 100 kHz was measured. For excitation (3) and measurement (7) we used the Solartron-system (2). Compared to the active electrode area of the needle the neutral electrode is much larger. Except for possible shortcomings of the setup when the distance d is very small (discussed in section 4), this ensures that the active electrode and its vicinity will contribute to the majority part of the system's impedance.

2.4. In vivo

To obtain unipolar measurements *in vivo* a three-electrode setup was used. A block diagram of this setup using a signal source (3) and an active operational amplifier (10) is shown in figure 2. The circuit gives a controlled potential between the active electrode (5) and the reference electrode (9) connected to the equipotential bulk tissue. By measuring (7) the current in the electrode lead (4) the impedance in the active electrode interface and the surrounding tissue can be determined without any influence from the reference or the current-carrying electrode (6) (Further described by Grimnes and Martinsen (2008) and Grimnes (1983), and also used by Morimoto *et al* (1990) and Salazar *et al* 2004)). In our measurements, we used the Solartron-system (2) for similar three-electrode measurements. The output port from the Solartron 1294 was connected to the needle (5) and the current-carrying electrode (6), to set up the excitation current through these electrodes. The sensing port was connected with one input on the needle (5) and one on the reference electrode (9). In this way, only the impedance between these electrodes is measured. Since no current is passing through the reference electrode, the EPI from this is eliminated from the measurements, and the measurements are consequently dominated by the properties of the active electrode and its surrounding tissue.

This setup was used to gather *in vivo* impedance data by measuring on an anesthetized pig (∼30 kg). The experiments/procedures have been approved by the approved competent person under the surveillance of the Norwegian Animal Research Authority (NARA) and registered by that Authority. Ag/AgCl electrodes ('Blue sensor' Q-00-A, Ambu Medicotest A/S DK) were placed on the skin and used as current (6) and reference (9) electrodes. The placement of these electrodes was done so that no unnecessary tissue series impedance was introduced. To ensure full contact, the skin was shaved before placement. Access to muscle, fat, spleen, liver, bile, urine and blood was obtained by cutting through the skin and placing the needles directly into the tissue. Needle placements were selected by an experienced surgeon so that the tissue around the needle tip was as homogenous as possible. The insertion depth was approximately 10 mm. The homogeneity of the tissue sample volume and the needle position was also ensured by ultrasound (GE Vingmed Ultrasound, System Five) operated by an experienced radiologist. Such measurements were done with placements of both needles in six samples of each tissue type. Exclusion criteria were that the ultrasound tissue characterization was uncertain or if any production error or damage was detected in the needle insulation. All needles were inspected before and after measurements.

2.5. Analysis

The statistical distribution of the measured *in vivo* impedance data was evaluated, and partial least-squares discriminate analysis (PLS-DA) was performed on a data set containing all *in vivo* measurement from both needle types. For these analyses we used the Unscrambler 9.7 software from Camo Inc.

3. Results

3.1. In vitro

The dependence between position and impedance in the *in vitro* measurements is shown in figure 3. The curve clearly shows that the modulus ($|Z|$) was almost independent of the position in the middle of the tank, but had abrupt changes near the top and bottom. Moving the needle from 0 to 2.6 mm up from the bottom increases the modulus from short circuit to 385 Ω. This corresponds to 97% of the 396 Ω modulus at 17 mm. A corresponding change is seen at needle positions near the saline surface, where the modulus increases as the needle is moving towards the high impedance air. A similar trend is seen in the phase angle, but with a more evident needle depth dependence in the middle depth range.

3.2. In vivo

In vivo impedance spectra for different placements in fat and muscle tissue measured with needle type 1 is plotted in figure 4. One needle of type 1 had insufficient insulation in the mounting point between the shaft and the upper part of the needle. The lack of insulation leads to an erroneous current path through the body fluid, when the needle was handled by wet operating gloves. The lack of insulation could easily be detected by visual inspection, but was discovered later as a conspicuous low-impedance measurement. Due to exclusion of these measurements, only four muscle measurements are plotted with the six measurements in fat. For frequencies above 200 kHz the modulus ($|Z|$) shows a clear separation between the tissue types. For the phase angle (θ) a similar result is seen between 20 and 100 kHz. The corresponding measurements with needle type 2 are plotted in figure 5. The separation in

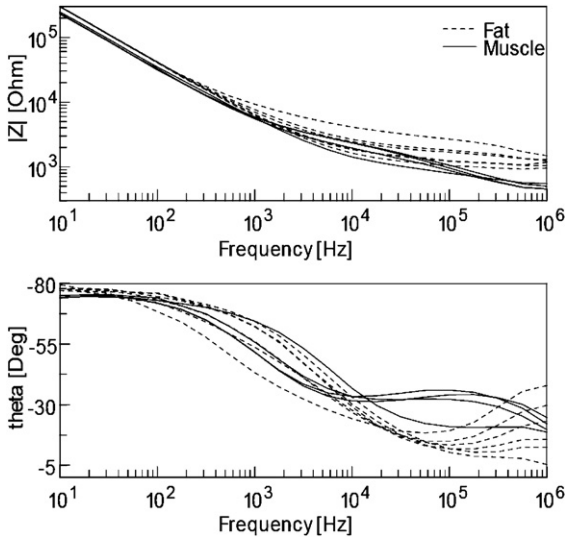

Figure 4. Complex impedance spectra measured with needle type 1 for six placements in fat and four placements in muscle tissue in a living pig.

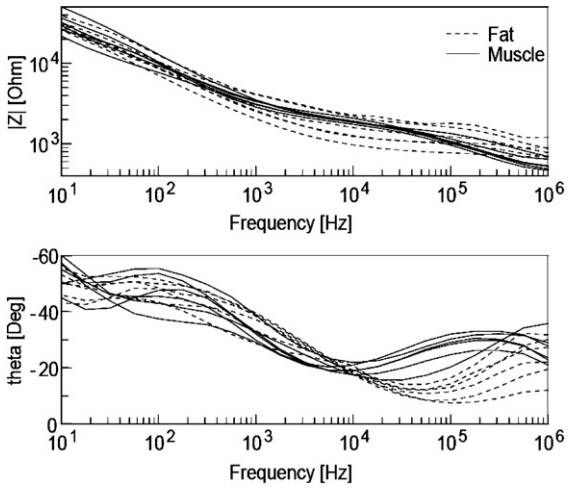

Figure 5. Complex impedance spectra measured with needle type 2 for six placements in fat and muscle tissue in a living pig.

the high-frequency (>200 kHz) modulus is not absolute with this needle, but the phase angle between 20 and 300 kHz shows sufficient discrimination for tissue characterization.

Typical spectra for all tissue types measured with needle type 1 are plotted in figure 6. From visual inspection the spectra have somewhat different patterns dependent on tissue type. Differences can be seen both in the modulus and phase.

3.3. Analysis

The measured resistance and reactance were found to be predominantly log-normal distributed and all statistical calculations were hence done on the logarithm of the resistance and reactance

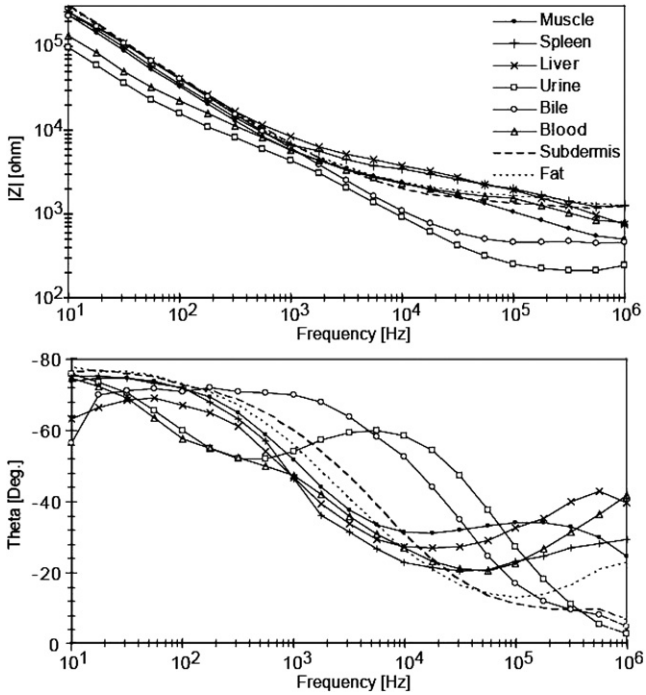

Figure 6. Impedance modulus ($|Z|$) and phase (θ) from measurements using needle type 1 in eight different tissues of a living pig.

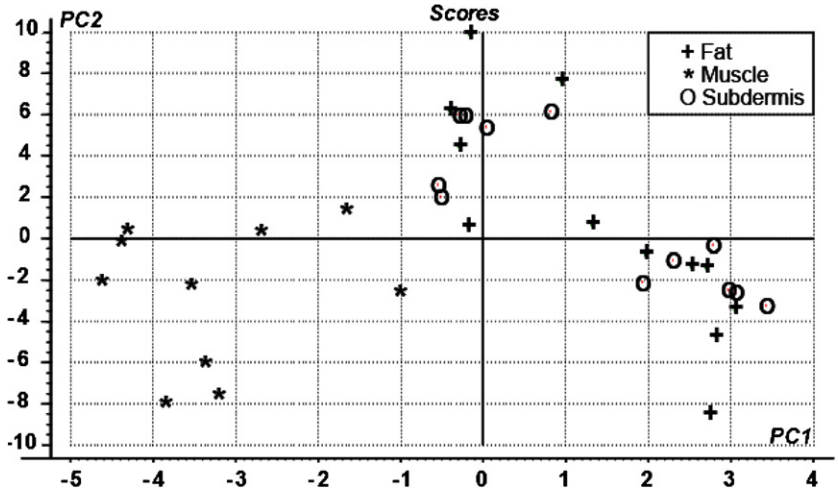

Figure 7. The scores plot from the PLS analysis by showing the first two principal components (PC1–PC2). The analyses were done in the 'Unscrambler® 9.7' software by using the logarithm of the resistance and reactance values from the measurement shown in figures 4 and 6. The plot indicates a clear separation of muscle tissue from fat and subdermis in this data set.

values. Figure 7 shows a scores plot from the classification, and for this data set it can readily be seen that a 100% separation between muscle tissue on one side, and subdermis and fat on the other side can be made. This is also obvious from the regression plot of figure 8.

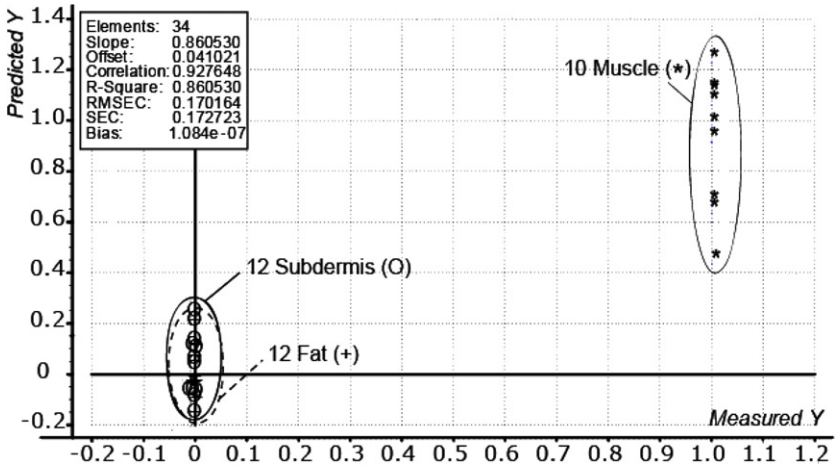

Figure 8. The plot shows the results from the regression analysis of the data from figure 7. The predictive model found in the 'Unscrambler® 9.7' software has a *Y* value above 0.4 for all muscle measurements, and below 0.3 for all fat and subdermis measurements. This gives a 100% separation of muscle for this data set.

4. Discussion

We have presented some results from a study concerning needle electrodes and tissue discrimination in a porcine model. To measure the electrical properties of a given type of tissue *in vivo*, we have to be certain that the measurements reflect the properties of this tissue alone and are not influenced by other adjacent tissues. Without proper knowledge of the sensitivity zone of the measuring system, we will not be able to pick a suited tissue volume for the measurements. To do this, we need to know the minimum homogenous tissue size and how far from the tissue boundaries the measuring electrode must be placed to eliminate the influence from other types of tissue. A calculation of volume sensitivity in such a system should be based on the local current density in the tissue (Grimnes and Martinsen 2008, equation 6.36, Malmivuo and Plonsey 1995). In a parallel study for later publication, we have developed a needle electrode model for this kind of sensitivity zone simulations. To determine the sensitivity zone of our measuring system, we have presented here results from one of the *in vitro* experiments done in this parallel study. Using this *in vitro* model we found that moving the needle 2.6 mm up from the bottom gave a change in the impedance modulus of about 97% compared to the modulus in the middle of the tank. We also found a corresponding change near the saline surface (figure 3). However, our *in vitro* model has some possible shortcomings. As the needle approaches the neutral electrode, a smaller area of the metal plate will contribute to the conduction. This will gradually change the setup to be more bipolar. When the needle is at 0 mm, the saline is short circuited, and we will not be able to measure on an ionic wet conductor as wanted. Also at the top of the saline bath, it is difficult to predict how the size of the active electrode area will depend on the distance from the bottom. We measured the length of the non-insulated needle tip to approximately 0.6 mm. So from 34.4 mm and up, parts of the electrode area may dry out. Both of these effects only appear at short distances compared to 2.6 mm. Compared to the theoretical calculation on a sphere (Cao *et al* 2002) and a hemisphere (Grimnes and Martinsen 2008), with a radius comparable to the length of our needle tip, this corresponds to a considerably smaller 90% sensitivity zone. But, due to the conical shape, the active area of our electrode was also considerably smaller than for such

a sphere or hemisphere, so this should be expected. The sensitivity is dependent on the square of the current density (Grimnes and Martinsen 2008), and a sharp needle will have the highest current density on the tip (Woo *et al* 2000). This will give an enhanced sensitivity in this area, and contribute to a smaller sensitivity zone for our needle compared to a smoother electrode surface on a sphere or hemisphere. Kinouchi *et al* (1997) used a conical needle for simulation. They only gave the diameter of their electrode, but from the scaling on their figure the needle tip length is about 2 mm. This gives an active electrode area of approximately 1.6 mm^2, which is roughly five times the area of our electrode. Hence, our measured sensitivity zone is in accordance with Kinouchi *et al* (1997). Furthermore, since these measurements were done with exactly the same type of needle as we use to gather the *in vivo* data, we can conclude that the major sensitivity of our needle type 1 electrode system will be within a sphere of a radius of 2–3 mm from the needle tip.

The phase angle measurements showed some dependence to the needle depth in the middle of the tank (figure 3). The properties of the needle insulation were evaluated by pilot measurement and theoretical calculation. From this we found that the depth dependence corresponded to the capacitive coupling through the needle insulation ((4) in figure 1). The insulation can be looked upon as a dielectric layer between the needle and the saline. Hence the capacitance is proportional to the contact area in the saline, and its influence is more pronounced at higher frequencies. Thus a high-frequency measurement of this capacitance will be dependent on the insertion depth. This enables the determination of the needle depth from our measuring method.

Some stainless steel alloys can change electrode properties after use (Schwan and Kay 1956, Dorfman *et al* 1985, Khambete *et al* 1995), so we had to test the electrodes we wanted to use. In pilot studies, the stability of both needle types was tested as a function of transferred current and tissue placement. The results showed that the needles of type 2 were very stable and had no noticeable change in these tests, but the impedance of needle type 1 was lowered after current transfer. The best result was obtained by preconditioning the needles of type 1 with a cathodic constant current of 1 μA in 1 min in a sterilized saline bath (0.9% NaCl). This lowered the impedance, and stable properties were ensured also for these needles. Further research is necessary to fully understand this process.

In figures 4 and 5 we found that characteristic tissue properties could be repeatedly measured in different samples of fat and muscle tissues. The two needle types have different electrode geometry which gives quite different electric properties, but still in both cases, characteristic differences between tissue types are revealed. Differences in measurements can be seen in the whole frequency range. Figures 4–6 show clear tissue dependence below the kHz range where measurements are dominated by EPI. These experimental results are in accordance with what Schwan (1992, 1966) found in the suspension. It also indicates that new interpretation of EPI data can be used to improve current methods for tissue discrimination. To utilize tissue discrimination based on EPI and tissue data we have also introduced multivariate analysis as a beneficial tool. Multivariate analysis has become a quite common tool for impedance data analysis, but has not been used earlier for needle guidance.

Single measurements from five tissues and three body fluids are plotted in figure 6. The spectrum from these tissue types shows considerable differences both in phase and modulus. A single spectrum gives no statistically significant indication, so measurements from up to 12 different placements in each tissue type are included in figure 7. In the plot, all measurements fall within their own unique tissue specific area. This is a good indication that an applicable separation algorithm for this kind of tissue data can be found. Our regression analysis, plotted in figure 8, shows a clear separation of muscle from fat and subdermis. In the plot, all muscle data have 'predicted Y' > 0.4 while the fat and subdermis data have 'predicted Y' < 0.3. Based

on this analysis a prototype discrimination algorithm was developed and tested with success in two other porcine model experiments. Further data gathering and analyses are currently done to develop such an algorithm with high accuracy for clinical use.

We have developed an algorithm focused on discrimination between tissue types based on tissue data including EPI. During this work, establishing a measuring cell constant to calculate specific tissue properties (Gabriel *et al* 1996b, Schwan 1963, 1966, Stoianovici *et al* 2002, Salazar *et al* 2004) is not necessary. But a reliability evaluation can be done in the high-frequency range where we have the least contribution form EPI. For both needles the muscle data have a clear drop in the modulus and at local maxima in the phase angle around 200 kHz. This is not seen in fat, and corresponds to the muscle tissue dispersion reported by others (Gabriel *et al* 1996a).

In our opinion, proper knowledge of measurement system sensitivity, new interpretations of EPI data and multivariate analysis will bring considerable contributions to impedance-based tissue discrimination for needle guidance or any other applications using such methods.

5. Conclusion

In a porcine model, we have shown that refined impedance-based needle guidance seems feasible with appropriate spatial resolution by using multivariate analysis, EPI influenced measurement data and needle electrodes with adapted size.

Acknowledgments

The authors would like to thank Axel Sauter for clinical assistance, and the Department of Comparative Medicine for support in animal care.

References

Cao H, Tungjitkusolmun S, Choy Y B, Tsai J Z, Vorperian V R and Webster J G 2002 Using electrical impedance to predict catheter-endocardial contact during RF cardiac ablation *IEEE Trans. Biomed. Eng.* **49** 247–53

Cheung P, Hall B, Chugh A, Good E, Lemola K, Han J, Tamirisa K, Pelosi F, Moray F and Oral H 2004 Detection of inadvertent catheter movement into a pulmonary vein during radiofrequency catheter ablation by real-time impedance monitoring *J. Cardiovasc. Electrophysiol.* **15** 674–8

Dalamagas P P and Sapia M A 1993 Method to sense the tissue for injection from a hypodermic needle *United States Patent no* 5,271,413 (Dec. 21)

Dorfman L J, McGill K C and Cummins K L 1985 Electrical properties of commercial concentric EMG electrodes *Muscle Nerve* **8** 1–8

Faes T, van der Meij H A, de Munck J C and Heethaar R M 1999 The electric resistivity of human tissues (100 Hz–10 MHz): a meta-analysis of review studies *Physiol. Meas.* **20** R1–10

Foster K R and Schwan H P 1995 Dielectric properties of tissue *Handbook of Biological Effects of Electromagnetic Radiation* 2nd edn, ed C Polk and E Postow (Boca Raton, FL: CRC Press) pp 25–102

Gabriel C, Gabriel S and Corthout E 1996a The dielectric properties of biological tissues: I. Literature survey *Phys. Med. Biol.* **41** 2231–49

Gabriel S, Lau R W and Gabriel C 1996b The dielectric properties of biological tissues: II. Measurements in the frequency range 10 Hz to 20 GHz *Phys. Med. Biol.* **41** 2251–69

Gordon M P J and Chandler N P 2004 Review: electronic apex locators *Int. Endod. J.* **37** 425–37

Grimnes S 1983 Impedance measurement of individual skin surface electrodes *Med. Biol. Eng. Comput.* **21** 750–5

Grimnes S and Martinsen Ø G 2008 *Bioimpedance and Bioelectricity Basics* 2nd edn (San Diego: Academic)

Hernandez D J, Sinkov V A, Roberts W W, Allaf M E, Patriciu A, Jarrett T W, Kavoussi L R and Stoianovici D 2001 Measurement of bio-impedance with a smart needle to confirm percutaneous kidney access *J. Urol.* **166** 1520–3

Johnson T C, Balbierz D J and Pearson R M 2003 Apparatus for detecting and treating tumours using localized impedance measurement *United States Patent no* US 2003/0109871 A1 (Jun. 12)

Khambete N D, Shashidhara J, Bhuvaneshwar G S and Sivakumar R 1995 Impedance measurement system for concentric needle electrodes *Proc. RC IEEE-EMBS and 14th. 1.1–1.2*

Kinouchi Y, Iritani T, Morimoto T and Ohyama S 1997 Fast *in vivo* measurements of local tissue impedances using needle electrodes *Med. Biol. Eng. Comput.* **35** 486–92

Levendusky J A, Rioux R F, Geitz K A E, Dodson S A and Rauker R M 2005 Apparatus with partially insulated needle for measuring tissue impedance *United States Patent no* US 2005/0288566 A1 (Dec. 29)

Malmivuo J and Plonsey R 1995 *Electroencephalography in Biomagnetism—Principles and Applications of Bioelectric and Biomagnetic Fields* (Oxford: Oxford University Press)

Mirtaheri P, Grimnes S and Martinsen Ø G 2005 Electrode polarization impedance in weak NaCl aqueous solutions *IEEE Trans. Biomed. Eng.* **52** 2093–9

Morimoto T, Kinouchi Y, Iritani T, Kimura S, Konishi Y, Mitsuyama N, Komaki K and Monden Y 1990 Measurement of the electrical bio-impedance of breast tumors *Eur. Surg. Res.* **22** 89–92

Salazar Y, Bragos R, Casas O, Cinca J and Rosell J 2004 Transmural versus nontransmural *in situ* electrical impedance spectrum for healthy, ischemic, and healed myocardium *IEEE Trans. Biomed. Eng.* **51** 1421–7

Schwan H P 1963 Determination of biological impedances *Physical Techniques in Biological Research* vol 6 ed W L Nastuk (New York: Academic) pp 323–407

Schwan H P 1966 Alternating current electrode polarization *Biophysik* **3** 181–201

Schwan H P 1992 Linear and nonlinear electrode polarization and biological materials *Ann. Biomed. Eng.* **20** 269–88

Schwan H P and Kay C F 1956 Specific resistance of body tissues *Circ. Res.* **4** 664–70

Stoianovici D, Kavoussi L R and Jackman M A S 2002 Surgical needle probe for electrical impedance measurements *United States Patent no* 6,337,994 B1 (Jan. 8)

Woo E J, Tungjitkusolmun S, Cao H, Tsai J Z, Webster J G, Vorperian V R and Will J A 2000 A new catheter design using needle electrode for subendocardial RF ablation of vetricular muscles: finite element analysis and *in vitro* experiments *IEEE Trans. Biomed. Eng.* **47** 23–31